RI 9296

REPORT OF INVESTIGATIONS/1990

PLEASE DO NOT REMOVE FROM LIBRARY

Mathematical Modeling of Spontaneous Heating of a Coalbed

By John C. Edwards

1910 ★ 80 YEARS ★ 1990

BUREAU OF MINES

UNITED STATES DEPARTMENT OF THE INTERIOR

U.S. Bureau of Mines
Spokane Research Center
E. 315 Montgomery Ave.
Spokane, WA 99207
LIBRARY

Mission: As the Nation's principal conservation agency, the Department of the Interior has responsibility for most of our nationally-owned public lands and natural and cultural resources. This includes fostering wise use of our land and water resources, protecting our fish and wildlife, preserving the environmental and cultural values of our national parks and historical places, and providing for the enjoyment of life through outdoor recreation. The Department assesses our energy and mineral resources and works to assure that their development is in the best interests of all our people. The Department also promotes the goals of the Take Pride in America campaign by encouraging stewardship and citizen responsibility for the public lands and promoting citizen participation in their care. The Department also has a major responsibility for American Indian reservation communities and for people who live in Island Territories under U.S. Administration.

Report of Investigations 9296

Mathematical Modeling of Spontaneous Heating of a Coalbed

By John C. Edwards

UNITED STATES DEPARTMENT OF THE INTERIOR
Manuel Lujan, Jr., Secretary

BUREAU OF MINES
T S Ary, Director

Library of Congress Cataloging in Publication Data:

Edwards, John C.
Mathematical modeling of spontaneous heating of a coalbed / by John C. Edwards.

p. cm.-(Report of investigations / United States Department of the Interior. Bureau of Mines)

Includes bibliographical references.

Supt. of Docs. no.: I 28.23:9296.

1. Coal-Combustion-Mathematical models. 2. Spontaneous combustion-Mathematical models. I. Title. II. Series: Report of investigations (United States. Bureau of Mines); 9296.

TN23.U43 [TP325] 622 s-dc20 [6221.8] 89-600273

CONTENTS

ILLUSTRATIONS

TABLES

UNIT OF MEASURE ABBREVIATIONS USED IN THIS REPORT

°C	degree Celsius	$g \cdot cm^{-3}$	gram per cubic centimeter
$cal \cdot cm^{-2} \cdot s^{-1}$	calorie per square centimeter per second	$g \cdot cm^{-1} \cdot s^{-1}$	gram per centimeter per second
$cal \cdot cm^{-3} \cdot s^{-1}$	calorie per cubic centimeter per second	$g \cdot cm^{-3} \cdot s^{-1}$	gram per cubic centimeter per second
$cal \cdot cm^{-1} \cdot s^{-1} \cdot K^{-1}$	calorie per centimeter per second per degree kelvin	$g \cdot mol^{-1}$	gram per mole
$cal \cdot cm^{-2} \cdot s^{-1} \cdot K^{-1}$	calorie per square centimeter per second per degree kelvin	h	hour
$cal \cdot g^{-1} \cdot K^{-1}$	calorie per gram per degree kelvin	in	inch
cal-mol^{-1}	calorie per mole	K	degree kelvin
cm	centimeter	$kcal \cdot g^{-1}$	kilocalorie per gram
cm^2	square centimeter	$kcal \cdot mol^{-1}$	kilocalorie per mole
cm^3	cubic centimeter	$kJ \cdot mol^{-1}$	kilojoule per mole
$cm \cdot s^{-1}$	centimeter per second	$K \cdot s^{-1}$	degree kelvin per second
$cm \cdot s^{-2}$	centimeter per second squared	L	liter
$cm^2 \cdot s^{-1}$	square centimeter per second	$L \cdot min^{-1}$	liter per minute
D	darcy	m	meter
$dyn \cdot cm^{-2}$	dyne per square centimeter	μm	micrometer
$erg \cdot K^{-1} \cdot mol^{-1}$	erg per degree kelvin per mole	$m \cdot s^{-1}$	meter per second
ft	foot	s	second
		W	watt
		$W \cdot cm^{-3}$	watt per cubic centimeter

MATHEMATICAL MODELING OF SPONTANEOUS HEATING OF A COALBED

By John C. Edwards[1]

ABSTRACT

To have the capability to predict the development of localized spontaneous heating within a porous coalbed that is subjected to forced air ventilation or in an otherwise quiescent environment in which buoyancy develops, the Bureau of Mines developed three time-dependent mathematical models, which were used to calculate the temperature increase associated with chemisorption of oxygen by the coal. In each model, spontaneous heating is driven by an Arrhenius first-order reaction between the oxygen and coal. Two models are two-dimensional, and one is one-dimensional. In the first two-dimensional model, a constant-velocity forced convection airflow is specified; and in the other, buoyant flow is allowed to develop in the absence of forced convection. The third model evaluates the airflow from Darcy's law and a specification of the pressure at the surface of a one-dimensional porous coalbed. Numerical computations demonstrated how each model could be used to predict the onset of spontaneous heating when the porous coalbed was subjected to constraints of an imposed internal heat source or a high-temperature airflow. The effects of particle size and coalbed compaction upon spontaneous heating were examined with the third model.

[1]Research physicist, Pittsburgh Research Center, Bureau of Mines, Pittsburgh, PA.

INTRODUCTION

A mathematical model of spontaneous heating within a bed of coal rubble enables the researcher to identify the significant parameters that influence the heating. In a spontaneous heating process, the heat liberated from the irreversible oxidation of crushed coal increases the rate of reaction between the oxygen and the coal surface. A hazard is posed when the heat production exceeds the heat dissipation. This self-heating process can ultimately result in coal combustion. The effect of forced convection in a one-dimensional model of coal that reacts with oxygen as a first-order Arrhenius reaction was modeled by Nordon (*1*).[2] That model was extended by Edwards (*2*) to include the detailed modeling of heat transfer within the coal particles. A two-dimensional model of natural buoyancy generated by an embedded heat source within an enclosed porous medium was developed by Young, Williams, and Bryson (*3*). They showed that a hot spot in a coal dump might generate sufficient natural convection within the coal dump to maintain a sufficient oxygen supply. Brooks and Glasser (*4*) modeled buoyant flow through a one-dimensional bed in which an Arrhenius reaction occurred, and steady-state solutions were developed that could be utilized to classify the coalbed as "safe" or "unsafe."

As part of its research program to develop criteria for predicting and preventing spontaneous combustion in mines, the Bureau of Mines has developed several mathematical models of the spontaneous heating of coalbeds.

Following upon the research reported in references 1 and 2, a two-dimensional transient mathematical model for spontaneous heating in coal rubble was developed. In the model, the coal rubble was stimulated thermally by an externally powered, embedded heat source. A constant airflow in the porous bed was assumed, and buoyancy was neglected. This model was applied to temperature measurements made in a porous coalbed.

Efforts reported in references 3 and 4 to account for buoyancy have been extended by the Bureau to include the Arrhenius reaction of oxygen with the coal in a partially enclosed container in which an externally powered heater is embedded. In this second model, a transient two-dimensional model for spontaneous heating, buoyancy generated the airflow through the porous coalbed in a Boussinesq approximation (*5*).

In addition to these two-dimensional models, a one-dimensional transient model for spontaneous heating in a porous coalbed was developed that determined the interstitial airflow from Darcy's law. As distinct from the first two models, an embedded heat source was not present. Instead, incident air and initial coalbed temperatures were at an elevated value (37° C). The air pressure boundary condition was evaluated from the average wind velocity. The model was used to analyze the effect of coal particle size and bed porosity on the tendency for self-heating.

Each of the models was developed into a FORTRAN computer program that can be used to evaluate the tendency for spontaneous heating under a variety of physical constraints. The bed properties such as permeability and porosity can be varied, as well as coal particle properties such as particle diameter and Arrhenius kinetics. The dimensions of the coalbed and strength of the heater are additional parameters subject to variation. The effect of the environment upon the self-heating is controlled through the boundary conditions.

FORCED CONVECTION THERMAL MODEL

An experimental program at the Bureau's Pittsburgh Research Center (PRC) evaluated the development of spontaneous heating within a porous bed of coal. Air was supplied at a low rate, approximately 30 $L \cdot min^{-1}$, to a 15-ton coalbed that had a void volume of 5.05×10^3 L. The coal particle diameters were less than 6 in (15.2 cm). An embedded heat source, controlled externally, stimulated the development of spontaneous heating within the coal. The results of the test are to be presented in a future Bureau report. The model presented in this section is based upon the design of the experimental test.

The experimental coalbed, which is 6 by 15 ft and cuboid in shape, is described by rectangular cartesian coordinates in three dimensions. In the absence of significant buoyancy forces, a two-dimensional approximation is useful. In this latter case, cylindrical coordinates are used.

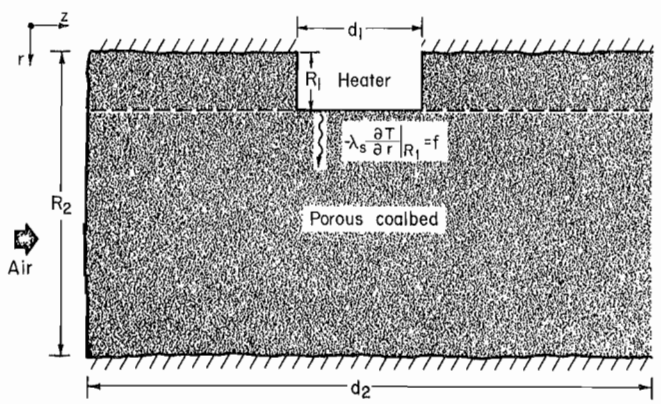

Figure 1.–Schematic of porous coalbed and embedded heat source for forced convection model.

[2]Italic numbers in parentheses refer to items in the list of references preceeding the appendix at the end of this report.

A schematic of the physical system represented in this model is shown in figure 1. A heating element of radius R_1 and length d_1 is embedded concentrically within a cylindrical coalbed of radius R_2 and length d_2. In the absence of buoyancy, which is a reasonable assumption if the forced convection is adequate to minimize the influence of the buoyant forces, the cylindrical symmetry of the system can be used in the development of the heat and mass transport equations. The coordinates are specified by radial coordinate r and axial coordinate z. (In the next section, "Buoyancy-Driven Thermal Model," a heat and mass transport model of spontaneous heating that includes buoyancy is presented.) The general development of the heat and mass transport equations in this section follows the presentation of Thorsness and Kang (*6*).

For the purpose of this simulation, the radius R_1 is an effective radius that is defined as the radius of an equivalent cross-sectional area of the two adjacent cylindrical heating pipes used in the experiment. This effective cross-sectional area is less than 4% of the cross-sectional area of the coalbed. The implication is that the heat and mass transfer in the region between R_1 and R_2 is more important than that occurring in front of and behind the heater element for radius r less than R_1. For this reason the inner axis of the cylindrical coalbed was selected at R_1. This improves the computational efficiency through the neglect of airflow around a convex boundary at the edge of the heater element at R_1.

Coal of average particle diameter d is packed in the bed with an interparticle bed porosity (void fraction) ϵ. At elevated temperatures the coal reacts with the oxygen in the air that flows through the bed. In accord with references 1-2 and 4, a first-order Arrhenius reaction rate is assumed. Transport of heat within the coalbed is assumed to obey the Fourier law of heat conduction, with an effective thermal conductivity defined according to Wakao and Kaguei (*7*, pp. 175-204). In the radial direction the effective thermal conductivity, $\lambda_r^{(e)}$ is defined by

$$\lambda_r^{(e)} = \lambda_o^{(e)} + 0.1\ \mathrm{Re}\ \mathrm{Pr}\ \lambda_g , \qquad (1)$$

and in the axial direction by

$$\lambda_z^{(e)} = \lambda_o^{(e)} + 0.5\ \mathrm{Re}\ \mathrm{Pr}\ \lambda_g , \qquad (2)$$

where Re = Reynolds number, $\frac{du\rho}{\mu}$;

Pr = Prandtl number, $\frac{\mu C_p}{\lambda_g}$;

d = particle diameter;

u = superficial gas velocity;

ρ = gas density;

μ = gas dynamic viscosity;

C_p = gas heat capacity;

and λ_g = gas thermal conductivity at temperature T.

Equations 1 and 2 decouple the effective thermal conductivity in the absence of flow, $\lambda_o^{(e)}$, from the contribution due to the flow.

The effective thermal conductivity $\lambda_o^{(e)}$ in the absence of flow is defined by

$$\lambda_o^{(e)} = \lambda_g \left[\frac{\lambda_s}{\lambda_g} \right]^{\alpha}, \qquad (3)$$

where $\alpha = 0.28 - 0.757 \log_{10}(\epsilon) - 0.057 \log_{10} \frac{\lambda_s}{\lambda_g}$,

and λ_s = particle thermal conductivity.

The temperature-dependent gas thermal λ_g is related to the gas thermal conductivity λ_{go} at ambient temperature T_o by

$$\lambda_g = \lambda_{go} \sqrt{\frac{T}{T_o}} . \qquad (4)$$

Mass diffusion of the oxygen becomes a significant factor in the control of the reaction process for low gas velocities as the reaction rate increases at high temperatures. The effective gas dispersion coefficients in the radial and axial direction, $D_r^{(e)}$ and $D_z^{(e)}$, are related to the molecular gas diffusion coefficients D_r and D_z, and the parameters ϵ, Re, Pr, and Sc. The parameter Sc is the Schmidt number, which is defined by

$$\mathrm{Sc} = \frac{\mu}{\rho D} . \qquad (5)$$

The functional dependence of $D_r^{(e)}$ and $D_z^{(e)}$ was determined by Bischoff (*8*) and Edwards and Richardson (*9*) for small particles.

$$D_r^{(e)}/D_r = 0.73\epsilon + 0.1\ \mathrm{Re}\ \mathrm{Sc} . \qquad (6)$$

$$D_z^{(e)}/D_z = 0.73\epsilon + 0.5\ (\mathrm{Re}\ \mathrm{Sc})^2/(9.7\epsilon + \mathrm{Re}\ \mathrm{Sc}) . \qquad (7)$$

It is assumed for this report that the chemisorption of oxygen by the coal particle surface is associated with a first-order Arrhenius reaction. This is not necessarily the case. Stott (*10*, p. 59) described the oxidation by a 0.5 power of the oxygen in the gas stream. The functional form of the first-order reaction rate $\dot{r}$, the rate of oxygen consumption, is

$$\dot{r} = \rho_1 \frac{\rho_s}{\rho_{10}} \frac{C_{ps}}{Q} (1-\epsilon)\ A\ e^{-E/RgT} \qquad (8)$$

where ρ_1 = mass density of the oxygen;

ρ_s = solid particle density;

ρ_{10} = oxygen mass density ambient conditions, = 0.24×10^{-3} g · cm^{-3};

C_{ps} = coal specific heat;

and Q = heat of reaction of oxygen with coal = 300 kJ · mol^{-1} O_2 reacted (= 2.24 kcal · g^{-1} O_2) (*10*).

The factor $(1-\epsilon)$ assures that in the absence of coal, no reaction occurs. The preexponential factor A and activation energy E were determined from an analysis of the rate of temperature rise in an adiabatic heating apparatus (*11*). The latter analysis observed that the heating rate $\frac{dT}{dt}$, measured in the adiabatic calorimeter test, can be fit to an Arrhenius heat rate expression:

$$\frac{dT}{dt} = Ae^{-E/RgT} \qquad (9)$$

Within the porous coalbed the oxygen mass density ρ_1 is determined from the transport equation that includes the irreversible processes of diffusion and chemical reaction. The oxygen transport equation is a partial differential equation in cylindrical spatial coordinates, and time.

$$\frac{\partial}{\partial t}\rho_1 + \frac{1}{r}\frac{\partial}{\partial r}(r\tilde{v}_r \rho_1) + \frac{\partial}{\partial z}(\tilde{v}_z \rho_1) = \frac{D_r^{(e)}}{\epsilon}\frac{1}{r}\frac{\partial}{\partial r}\left(r\rho \frac{\partial}{\partial r}\left[\frac{\rho_1}{\rho}\right]\right) + \frac{D_z^{(e)}}{\epsilon}\frac{\partial}{\partial z}\rho\frac{\partial}{\partial z}\left[\frac{\rho_1}{\rho}\right] - \frac{\dot{r}}{\epsilon}, \qquad (10)$$

where r = radial coordinate,

z = axial coordinate,

and $\tilde{v}_r$ and $\tilde{v}_z$ = radial and axial components of the interstitial gas velocity.

The total gas density is determined from the ideal gas law, with the assumption that the pressure remains nearly constant at the ambient pressure, P_o.

$$\rho = \frac{W}{R_g}\frac{P_o}{T}, \qquad (11)$$

where R_g = gas constant, 8.3143×10^7 erg · K^{-1} · mol^{-1},

and W = molecular weight of air, 29 g · mol^{-1}.

The interstitial gas velocity components $\tilde{v}_r$ and $\tilde{v}_z$ are related to the superficial gas velocity components v_r and v_z.

$$\tilde{v}_r = v_r/\epsilon \; ; \qquad (12)$$

$$\tilde{v}_z = v_z/\epsilon \; . \qquad (13)$$

In the model calculations presented here, $v_r = 0$ and v_z is constant.

The local gas temperature T and local average coal particle temperature T_s define the energy transport equation for the gas-solid system. The thermal transport equation is written in cylindrical coordinates.

$$\epsilon\rho C_p\frac{\partial T}{\partial t} + (1-\epsilon)\rho_s C_{ps}\frac{\partial T_s}{\partial t} + \rho C_p v_r + \frac{\partial T}{\partial r} + \rho C_p v_z \frac{\partial T}{\partial z} = \lambda_r^{(e)}\left(\frac{\partial^2 T}{\partial r^2} + \frac{1}{r}\frac{\partial T}{\partial r}\right) + \lambda_z^{(e)}\frac{\partial^2 T}{\partial z^2} + \dot{r}Q, \qquad (14)$$

where ρ_s = mass density of the coal particle.

Thermal transfer between the particles and the gas is governed by a linearized equation that is an application of Newton's law of cooling (heating).

$$\rho_s C_{ps}\frac{\partial T_s}{\partial t} = \frac{3h}{R}(T - T_s), \qquad (15)$$

where h = heat transfer coefficient, λ_s/R,

and R = average coal particle radius.

It is assumed that the coal particles equilibrate faster than changes in the coal particle environment, and therefore, the coal particles are assumed to be individually at a uniform temperature. For an average particle diameter of 7.6 cm, the coal particle equilibration time is approximately 2.6 h.

In the absence of the effective thermal conduction term and the reaction rate term in equation 14, equations 14 and 15 reduce to the Schumann model (7, p. 245). Schumann's model assumes the dominant modes of heat transfer are convection and heat transfer between the air and the solid particles.

The boundary conditions are based upon a specification of ρ_1, T, and T_s at the entrance, and a continuity of these dependent variables at the exit and along the solid boundary, as well as along the symmetry boundary at $r = R_1$. Along the heater surface, the thermal flux f, the electrical power supplied to the heater divided by the heater surface area, is conducted into adjacent solid material and satisfies Fourier's law of heat conduction.

$$-\lambda s\frac{\partial T}{\partial r}\bigg|_{R_1} = f. \qquad (16)$$

The inlet air temperature is set equal to 15° C, and the inlet oxygen mass density to 0.24×10^{-3} g·cm^{-3}.

Under the most general conditions, equations 10, 14, and 15 do not yield an analytic solution. For this reason, a numerical procedure was adapted to solve these partial differential equations in a finite difference representation. The finite difference equations are implicit in time, and a central difference representation was used for the spatial derivatives. The resultant coupled nonlinear algebraic equations are solved iteratively. This was accomplished with a FORTRAN computer program.

Physical property values are listed in table 1 for the solid coal particles and the gas. For the computations considered herein: R_1 = 13.4 cm, R_2 = 68.8 cm, d_1 = 104 cm, and d_2 = 240 cm. In the model, the heating source is located 32 cm from the entrance to the coal region. It is assumed that the convective transport of the air prevents an upstream influence of the localized heating upon the temperature of the coalbed entrance, and that the temperature rise is localized about the heating element, for the time of reaction considered. The assumption of localized heating, which was validated in the calculations, permitted the utilization of values of R_2 and d_2 that were significantly less than the experimental coalbed dimensions.

Table 1.–Physical properties of coal and gas

Particle thermal conductivity (λ_s) . . cal·cm^{-1}·s^{-1}·K^{-1} . .	4.78 x 10^{-4}
Molecular gas thermal conductivity at ambient temperature (λ_{go}) . . . cal·cm^{-1}·s^{-1}·K^{-1} . .	6.0 x 10^{-5}
Solid particle density (ρ_s) . . . . . g·cm^{-3} . .	1.3
Molecular gas diffusion coefficient (D) . . . cm^2·s^{-1} . .	0.15
Porosity (ϵ)	0.33
Gas specific heat (C_p) . . . . . cal·g^{-1}·K^{-1} . .	0.24
Coal specific heat (C_{ps}) . . . . . cal·g^{-1}·K^{-1} . .	0.24
Gas dynamic viscosity (μ) . . . . . g·cm^{-1}·s^{-1} . .	1.8 x 10^{-4}
Coal particle diameter (d) . . . . . cm . .	7.62

Values used for the activation energy E and preexponential factor A were determined from adiabatic calorimeter tests for a high-volatile C bituminous coal.[3] The reactivity of the coal was defined by a value of E = 21.5 kcal·mol^{-1} and A = 0.123×10^{10} K·s^{-1}. The preexponential factor A was determined in the adiabatic calorimeter test for coal particles with diameters between 75 and 150 μm. This factor is assumed to be inversely proportional to the particle size (*4*). For the calculations considered in this section, the preexponential factor associated with 7.6-cm-diameter particles was utilized.

Figure 2 shows, for a fixed superficial air velocity (axial component) of 0.03 cm·s^{-1} and four distinct power levels

[3] Tests done by A. C. Smith, research chemist, Pittsburgh Research Center.

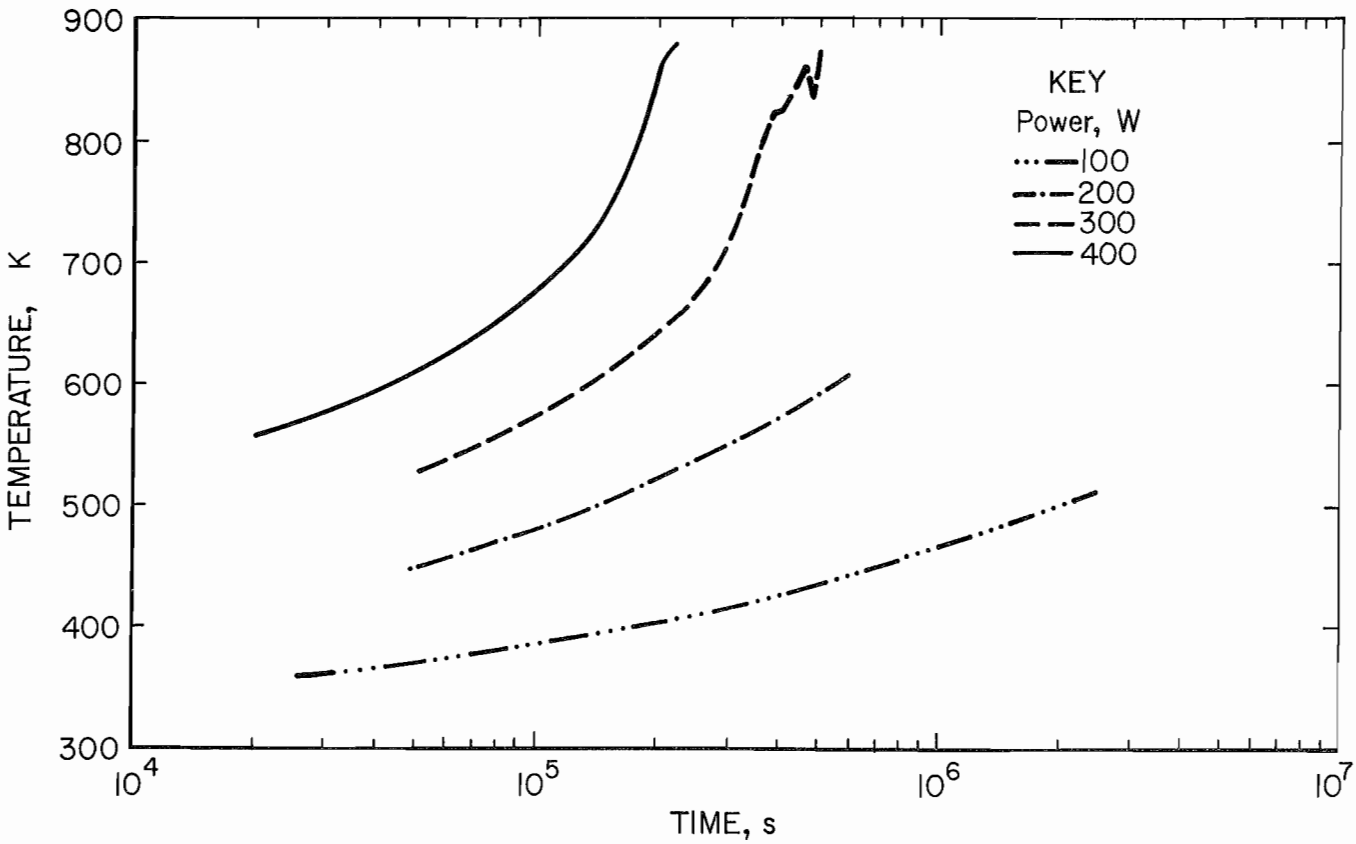

Figure 2.–Calculated time-dependent gas temperature at heater element in coalbed for power source of 100, 200, 300, and 400 W and superficial air velocity axial component of 0.03 cm·s^{-1}.

of 100, 200, 300, and 400 W, the time-dependent predicted maximum gas temperature at the heater surface. A superficial air velocity axial component twice the experimental value of 0.015 cm · s^{-1} was used to accelerate the computational speed. For the calculations presented in this section, radial airflow was neglected. The model equations as employed are two dimensional only with respect to thermal and mass diffusion. The effect of air speed upon the heating of the coalbed is shown in a subsequent calculation. As expected, the rate of temperature rise is influenced by the strength of the heat source. The nonmonotonic behavior that occurs in the curve for a 300-W power source at high temperatures is attributed to the oxygen depletion. (The location of the shown maximum temperature is shifted in the coalbed through the competing effects of chemical reaction, forced convection, and oxygen diffusion.) The temperature-time curves in figure 2 for 300- and 400-W power sources clearly show the rise in temperature that occurs at an increasingly rapid rate with respect to time. Excessive localized heating is not dissipated as rapidly as it is produced, and a condition known as thermal runaway ensues.

The results in figure 2 are as expected. An increase in the power from the heat source results in an increase in the heating rate of the coalbed adjacent to the heater and an increase in the gas temperature within a shorter period of time. The calculated nonlinear dependence of temperature rise upon power source over a period of time shows the advantage of a numerical model for predicting the effect of spontaneous heating in a coalbed. At the elevated temperatures shown, buoyancy becomes a significant factor; it is considered in the next section.

Figure 3 shows the effect of convection upon the heating of the coalbed with a 300-W power source. An increase in the superficial air speed from 0.03 to 0.06 cm · s^{-1} had no appreciable effect upon the heating for time less than 0.3×10^6 s.

The spontaneous heating model was used to analyze temperature measurements in a coalbed utilized in a

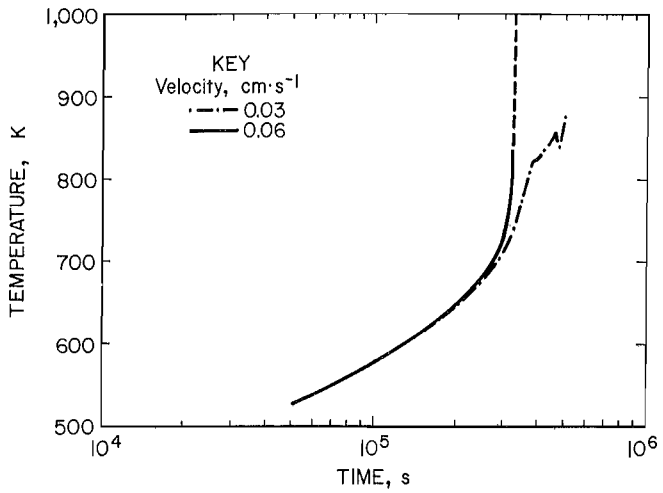

Figure 3.–Calculated time-dependent gas temperature at heater element in coalbed for power source of 300 W and superficial air speeds of 0.03 and 0.06 cm · s^{-1}.

spontaneous heating experiment at PRC.[4] The temperature rise at the heater surface was a measured quantity over a 40-day period (fig. 4). This measured temperature was used as a time-dependent boundary condition that replaced equation 16. An application of equations 10-16, along with this boundary condition on the approximate temperature at the heater surface, resulted in the predicted temperature evolution 15 cm distant from the midlocation of the heater, shown in figure 4. The predicted temperature is in substantial agreement with the measured temperature 15 cm below the heater. For this calculation, the experimental superficial air velocity of 0.015 cm · s^{-1} was used.

After 40 days, the power to the heater was disconnected. The temperature 15 cm below the heater achieved a maximum of 225° C within a week, and then decreased. This was not observed in the calculated results.

[4]Tests done by A. C. Smith, research chemist, Pittsburgh Research Center.

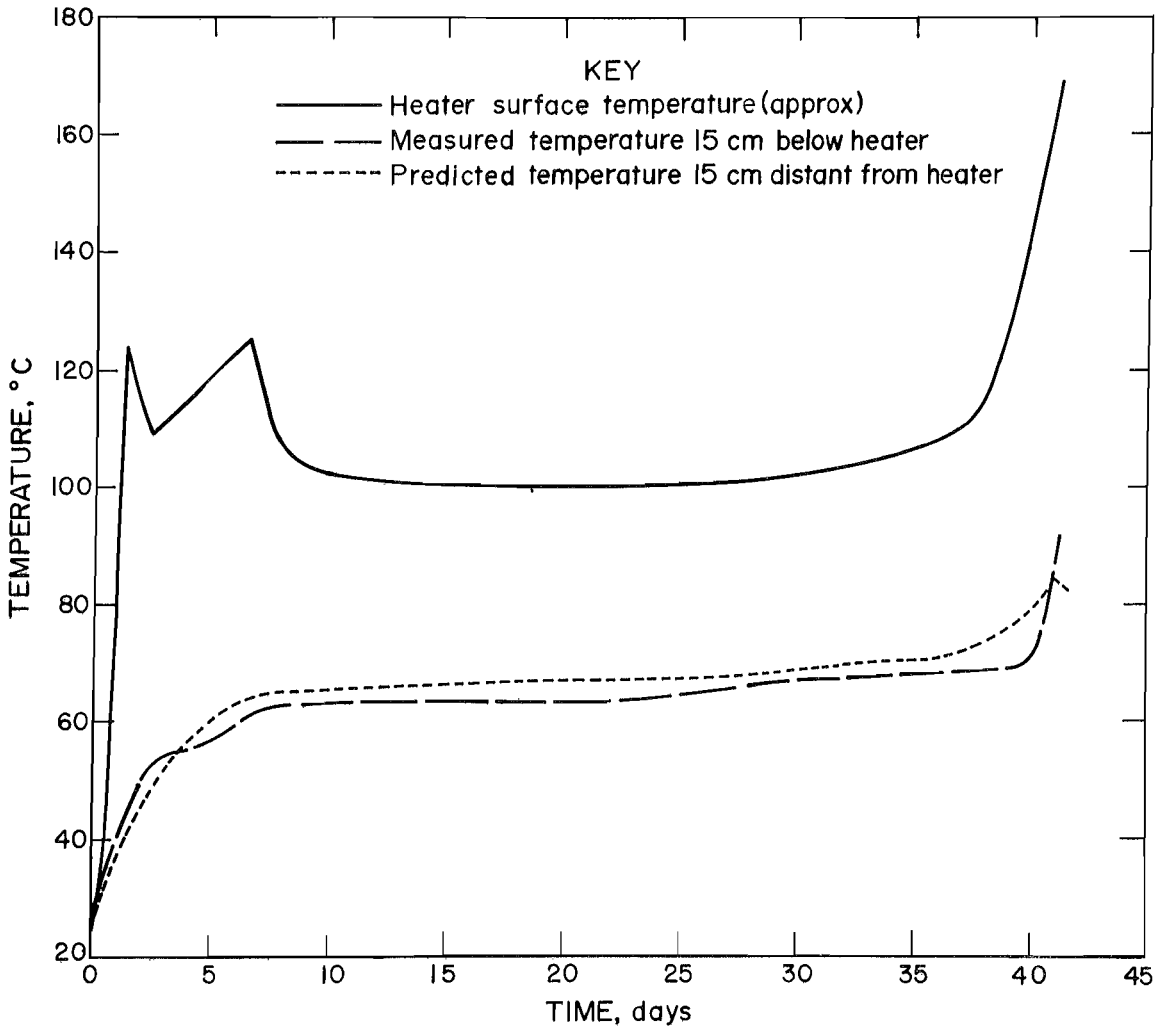

Figure 4.–Measured and predicted temperatures 15 cm from heater for a measured heater surface temperature.

BUOYANCY-DRIVEN THERMAL MODEL

A second thermal model of spontaneous heating was developed in order to analyze heating within a porous coalbed in which buoyancy of the heated gas is the principal mode of convective heat transfer. Figure 5 shows a schematic of the coalbed and the region heated by an externally controlled embedded power source. The rectangular enclosure is open on the right, through which the buoyancy force causes an exchange of air with the ambient environment.

This three-dimensional problem is reduced to a two-dimensional one in rectangular coordinates with the assumption that heat and mass transfer normal to the walls is not significant in comparison with that in the longitudinal and transverse directions denoted by x and y in figure 5. The enclosure will impose recirculation patterns on the airflow.

The transport equations for oxygen density, total gas density, and temperature in two-dimensional rectangular

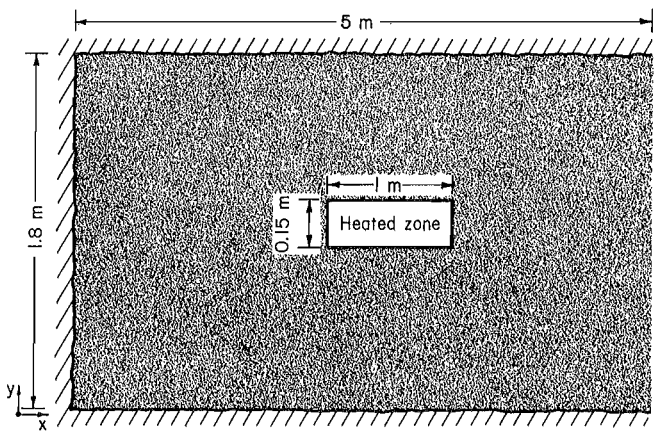

Figure 5.–Schematic of partially enclosed porous coalbed and embedded heat source for buoyancy-driven thermal model.

coordinates (x, y), as shown in figure 5, are nonlinear partial differential equations.

The oxygen species density ρ_1 satisfies

$$\frac{\partial \rho_1}{\partial t} + \frac{\partial}{\partial x}(\rho_1 \tilde{v}_x) + \frac{\partial}{\partial y}(\rho_1 \tilde{v}_y) = \frac{D_x^{(e)}}{\epsilon} \rho \frac{\partial^2}{\partial x^2}\left[\frac{\rho_1}{\rho}\right]$$

$$+ \frac{D_y^{(e)}}{\epsilon} \rho \frac{\partial^2}{\partial x^2}\left[\frac{\rho_1}{\rho}\right] - \frac{\dot{r}}{\epsilon} . \qquad (17)$$

The longitudinal coordinate is x, and the transverse coordinate is y. The dispersion coefficients $D_x^{(e)}$ and $D_y^{(e)}$ are evaluated as counterparts to equations 6 and 7 with a correspondence between the coordinates (x, y) and (z, r).

The total gas density ρ satisfies

$$\frac{\partial}{\partial t}\rho + \frac{\partial}{\partial x}(\tilde{\rho v}_x) + \frac{\partial}{\partial y}(\tilde{\rho v}_y) = -\frac{\dot{r}}{\epsilon} , \qquad (18)$$

where the loss of oxygen is through chemisorption on the coal particle surface with, in the early stage of spontaneous heating, negligible addition of gases from the coal particles.

The gas temperature T satisfies

$$\frac{\partial T}{\partial t} + \tilde{v}_x \frac{\partial T}{\partial x} + \tilde{v}_y \frac{\partial T}{\partial y} = \frac{\lambda_x^{(e)}}{\epsilon \rho C_p} \frac{\partial^2 T}{\partial x^2} + \frac{\lambda_y^{(e)}}{\epsilon \rho C_p} \frac{\partial^2 T}{\partial y^2}$$

$$- \frac{3h}{R \rho C_p} \frac{1-\epsilon}{\epsilon}(T-T_s) + \frac{\dot{r}Q}{\rho C_p \epsilon} + \frac{S}{\rho C_p \epsilon} . \qquad (19)$$

The thermal conductivities $\lambda_x^{(e)}$ and $\lambda_y^{(e)}$ are evaluated as counterparts to $\lambda_z^{(e)}$ and $\lambda_r^{(e)}$ of equations 1 and 2.

The thermal history of the solid matrix through which the air flows is governed by equation 15.

The source term S defines the power added to the system in the heated region. It is assumed power is uniformly added to the localized region in figure 5 that is designated "heated zone." The source strength S is defined in terms of the power P_w (watts) distributed over the volume V of the heated region consisting of two parallel heater rods of radius R_o = 7.5 cm and length d_1 = 1 m.

$$S = P_w / 4.184V , \qquad (20)$$

where $V = 2\pi R_o^2 d_1$.

For computational simplicity, it is assumed that the heated zone is permeable to airflow. A value of P_w equal to 200 W was used for this calculation.

The gas flow through the porous coalbed is developed from the momentum equations in a steady-state approximation for Boussinesq flow in a similar manner to the presentation in reference 3.

$$\frac{\partial P}{\partial x} = -\frac{\mu}{k} v_x , \qquad (21)$$

$$\frac{\partial P}{\partial y} = -\frac{\mu}{k} v_y + g\rho_o \frac{T-T_o}{T} , \qquad (22)$$

where μ = gas dynamic viscosity,

ρ_o and T_o = ambient gas density and temperature,

g = acceleration due to gravity,

and k = permeability of coalbed.

The ambient temperature was 15° C, and the ambient gas density was 1.2×10^{-3} g·cm^{-3}.

If the gas flow adjusts rapidly to temperature changes within the coalbed, then a quasi steady-state approximation in which the gas flow is calculated at the end of each time interval is a valid approximation. This approximation deteriorates as the spontaneous heating proceeds toward the onset of combustion, which occurs at about 500° C. Since the emphasis in this report is upon spontaneous heating, and not combustion, this quasi steady-state approximation is used. In a quasi steady-state approximation for the gas flow, the mass flux can be defined in terms of a stream function, Ψ.

$$\rho v_x = -\frac{\partial \Psi}{\partial y} ; \qquad (23)$$

$$\rho v_y = \frac{\partial \Psi}{\partial x} . \qquad (24)$$

Equations 21-24 are combined to eliminate the pressure. The resultant equation is

$$\frac{\partial^2 \Psi}{\partial x^2} + \frac{\partial^2 \Psi}{\partial y^2} - \frac{1}{\rho}\left[\frac{\partial \Psi}{\partial y}\frac{\partial \rho}{\partial y} + \frac{\partial \Psi}{\partial x}\frac{\partial \rho}{\partial x}\right] \qquad (25)$$

$$= g\frac{k\rho}{\mu}\frac{\rho_o T_o}{T^2}\frac{\partial T}{\partial x} .$$

For a constant total gas density, equation 25 reduces to a Poisson equation.

For coal particles in the porous bed with nonuniform diameters less than 15.2 cm, the gas permeability in the bed will be nonuniform. It is reasonable to expect that

the airflow in the bed will be controlled by regions with a permeability less than the median permeability of the coalbed. In the application of equations 21 and 22, an effective, constant permeability is used. A lower estimate for the permeability might be a value similar to that for soil. Soil is reported (*12*) to have a permeability within a range of 0.29 to 14 D. For this reason, a permeability of 10 D is used for an initial calculation.

Values used in the previous section for the preexponential factor and activation energy, as well as the physical constants in table 1, are used in the calculation presented here.

Equation 25 is solved numerically for Ψ with a central finite difference approximation used to replace the first and second partial derivatives. Values of ρ and T determined from the solution to the finite difference representation of equations 17-19 at a specific time step are used in the evaluation of Ψ. The new values of Ψ are used to define the gas flow at the next time step through an application of equations 23-24.

Since spontaneous heating was the subject of the study, the porous coalbed was kept from reaching the combustion temperature by turning off the heat source, S, whenever the temperature interior to the heated region exceeded 230° C. This provided an effective method of stimulating spontaneous heating, yet avoiding a transition to combustion.

Figure 6 shows the pattern of gas flow developed within the porous bed by the buoyancy forces generated by the temperature gradient in the gravitational field. The effect of the buoyancy is to induce recirculation within the porous bed. Air is drawn in at the bottom of the opening on the right side and expelled through the top of the opening on the right side.

Figure 7 shows the gas temperature, and oxygen density normalized by the oxygen density at the inlet, across the heated zone at the midheight of the heated zone after 1.47 h has elapsed. Because the heat source was suppressed whenever the local temperature exceeded 230° C, there was not any significant temperature change after 1.47 h. As expected, the normalized oxygen concentration achieves a minimum in the region of maximum temperature. The elevated temperature provides the driving force for the airflow patterns shown in figure 6.

The above calculation was repeated with an increase in the permeability to 3×10^6 D, which is characteristic of 7.6-cm-diameter particles, according to the Blake-Kozeny equation (*13*). The increased permeability resulted in greater air circulation. After 11.5 days had elapsed, the calculated interstitial air speed reached a maximum of 8 $cm \cdot s^{-1}$, compared with 10^{-3} $cm \cdot s^{-1}$ for the less permeable 10-D case. As a result of the increased air circulation, the maximum temperature reached 111° C after 11.5 days,

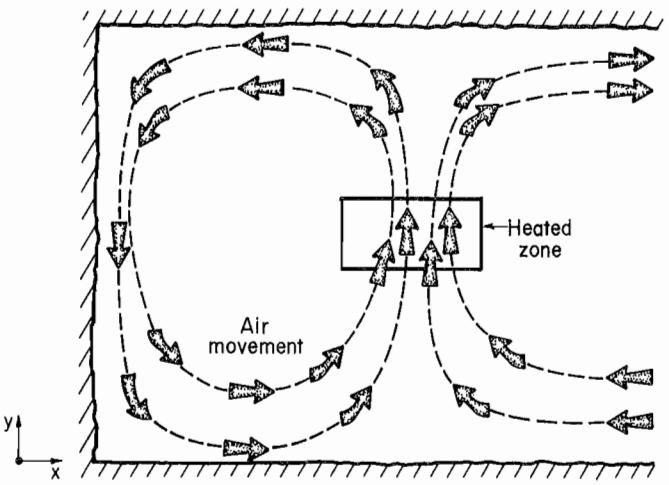

Figure 6.–Schematic of pattern of airflow associated with buoyancy-driven thermal model within partially enclosed porous coalbed.

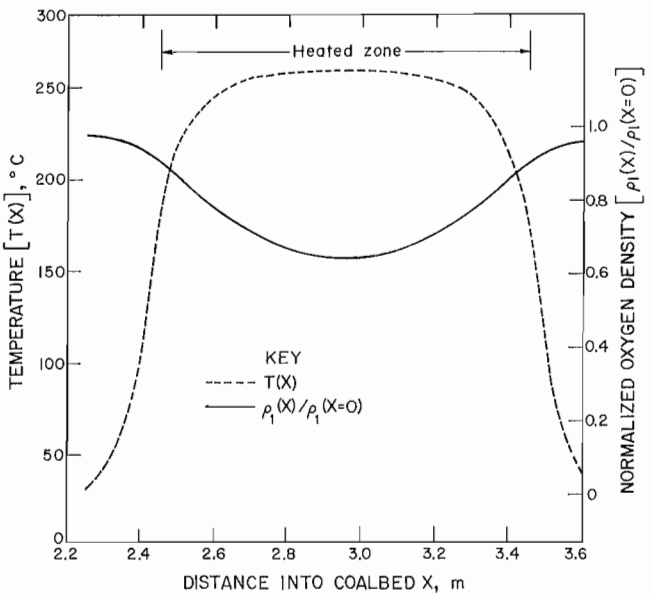

Figure 7.–Calculated air temperature and normalized oxygen density across midheight of heated zone in buoyancy-driven thermal model.

compared with 260° C after 1.47 h in the less permeable case. This comparison shows that the restriction to airflow imposed by the lower permeability prevents the adequate dissipation of heat by convection from a region of localized heating. The increased permeability, although moderating the rate of temperature rise, does not prevent spontaneous heating.

WIND-DRIVEN CONVECTION MODEL

A permeable coalbed impacted on one surface by wind will develop internal air currents as a result of the pressure differential established across the bed. This could occur for a coal pile exposed to a wind produced by the atmosphere or to ventilation in the exposed gob area of a mine. In this section, a permeable pile of coal is

represented by a one-dimensional coalbed. The single dimension is in the direction of the air pressure variation. Buoyancy is neglected in comparison with the forced convection. The gas pressure P at a distance x from the exposed surface of the bed, controlled by heat released through the chemisorption of oxygen on the coal particle surface as well as the air pressure at the bed boundaries, defines the interstitial gas velocity, $\tilde{v}$, through an application of Darcy's law.

$$\tilde{v} = -\frac{k}{\epsilon\mu}\frac{\partial P}{\partial x}. \tag{26}$$

The permeability is calculated from the Blake-Kozeny equation (*13*) for laminar flow through a porous bed.

$$k = \frac{d^2\epsilon^3}{150(1-\epsilon)^2}. \tag{27}$$

The driving gas pressure at the upwind face of the coalbed is determined from the conservation of mechanical energy. For a wind velocity w and inlet air density $\rho(x=o)$, the excess air pressure at the bed face over ambient is $0.5\ \rho(x=o)w^2$.

The appropriate transport equation for the oxygen of density ρ_1 within the permeable one-dimensional coalbed is

$$\frac{\partial}{\partial t}\rho_1 + \frac{\partial}{\partial x}(\rho_1\tilde{v}) = \frac{D^{(e)}}{\epsilon}\rho\frac{\partial^2}{\partial x^2}\left(\frac{\rho_1}{\rho}\right) - \frac{\dot{r}}{\epsilon}; \tag{28}$$

and the transport equation for the total gas species of density ρ is

$$\frac{\partial}{\partial t}\rho + \frac{\partial}{\partial x}(\rho\tilde{v}) = -\frac{\dot{r}}{\epsilon}. \tag{29}$$

Equation 8 defines the reaction rate $\dot{r}$.

For a conservative estimate (i.e., an underestimate) of the time required for spontaneous heating to become significant, the gas and solid particles are assumed to be in thermal equilibrium. Therefore, the energy transport equation is written as

$$(\epsilon\rho C_p + (1-\epsilon)\rho_s C_{ps})\frac{\partial T}{\partial t} + \rho C_p v\frac{\partial T}{\partial x} = \lambda^{(e)}\frac{\partial^2 T}{\partial x^2} + \dot{r}Q. \tag{30}$$

The gas pressure P is determined from ρ and T by the ideal gas equation of state.

$$P = \frac{R_g}{W}\rho T. \tag{31}$$

At the inlet to the permeable coalbed the appropriate boundary conditions are

$$P(x=0) = P_o + 1/2\ \rho(x=0)w^2, \tag{32}$$

$$\rho(x=0) = (P(x=0)/P_o)\ (T_o/T_1), \tag{33}$$

$$\rho_1(x=0) = 0.2\ \rho(x=0), \tag{34}$$

and $$T(x=0) = T_1, \tag{35}$$

where T_1 = inlet air temperature,

and T_o and P_o = ambient temperature and pressure.

At the exit to the permeable coalbed of length d_2 the appropriate boundary conditions are

$$P(x=d_2) = P_o, \tag{36}$$

$$\frac{\partial\rho}{\partial x} = 0 \text{ at } x = d_2, \tag{37}$$

$$\frac{\partial\rho_1}{\partial x} = 0 \text{ at } x = d_2, \tag{38}$$

and $$T(x=d_2) = \frac{w}{R_g}\frac{P_o}{\rho(x=d_2)}. \tag{39}$$

Equations 28-30 are coupled nonlinear partial differential equations. The method of numerical solution was to express these equations as algebraic equations with a backwards-implicit finite difference scheme. The resultant equations were solved with an application of the Newton-Raphson method at each spatial node throughout the one-dimensional packed bed over a finite time interval. The process was applied iteratively along with the boundary conditions until a converged solution was achieved. When convergence was achieved, the dependent variables ρ_1, ρ, T, P, and $\tilde{v}$ generated at the advanced time throughout the coalbed replaced their values at the previous time.

Several parametric studies were made with the model equations. The kinetics for another high-volatile C bituminous coal were used.[5] The preexponential factor was $0.596 \times 10^8\ K \cdot s^{-1}$, and the activation energy was 18.3 $kcal \cdot mol^{-1}$. Since the kinetic constants were determined for coal particles that ranged from 75 to 150 μm in diameter, the preexponential factor was determined for various particle diameters in this section by scaling A with the ratio 0.01125/d. This ratio is based upon an approximate average particle diameter of 112.5 μm as characteristic of the coal sample that determined A from the adiabatic calorimeter tests.

[5]Tests done by A. C. Smith, research chemist, Pittsburgh Research Center.

In order to reduce the computational time for a parametric study, an elevated temperature of 37° C was assigned to the air flowing into the coalbed and to the initial temperature of the coalbed. The ambient temperature was 15° C and the ambient pressure was 1.01325×10^6 dyn · cm^{-2}. The general trend that occurs in the development of spontaneous heating of a coal pile can be seen in the calculated bed temperature and oxygen concentration normalized by the oxygen concentration at the inlet, after localized heating has developed within the pile. In order to clarify the effects of the coupled physical processes of heat and mass transport and coal reactivity, yet maintain a reasonable computational time, calculations were made for porous coalbeds composed of 56.25-, 112.5-, and 225-μm-diameter coal particles. For a permeable coalbed 10 m in length, composed of coal particles of 56.25-μm diameter and an interparticle porosity of 0.33, and exposed at the surface to an incident wind with a speed of 2.2 m · s^{-1} and temperature of 37° C, the calculated coalbed temperature and normalized oxygen density shown in figure 8 develop after 35 days. Unless otherwise stated, all calculations in this section are for a 10-m-long bed, a bed porosity of 0.33, and an external wind velocity of 2.2 m · s^{1}. The calculated bed permeability is 1.69 D. Figure 8 shows that the gas temperature reaches a relative maximum value of 81° C at a distance 0.3 m into the bed. The normalized oxygen density decreases rapidly near the entrance to the coal pile.

Several observations are in order regarding a parametric study made of the influence of wind speed, bed porosity, and particle size on the spontaneous heating of the coalbed. It was established from a comparison of the calculated temperature internal to the coalbed that a change in the wind velocity from 2.2 m · s^{-1} to 4.4 m · s^{-1} had no significant effect upon the calculated thermal history of a coalbed composed of 112.5-μm-diameter particles for a 25-day time period. A maximum calculated bed temperature of 47° C was reached at the end of the 25-day time period.

Initially, the convective airflow induced by the pressure differential across the bed dominates. However, as self-heating, characteristic of the reaction kinetics and model equations, moves into dominance, the heat release produces internal pressures that compete against the externally applied pressure differential, and new interstitial airflows are established. The interstitial air speed induced in the coalbed by the wind that impacts upon the coalbed is of the order 10^{-5} cm · s^{-1} for wind speeds of 2.2 m · s^{-1}. This is in contrast to the interstitial air speed of 10^{-2} cm · s^{1} induced by the internal pressures generated by the heat released.

The coalbed porosity defines the degree of coalbed compaction. An increase in bed compaction is associated with a decrease in bed porosity. The bed porosity directly influences the bed permeability, equation 27, and several terms in the model equations, equations 28-32. The calculation shown in figure 8 for a coalbed 10 m in length composed of 56.25-μm-diameter particles for a bed porosity of 0.33 was repeated for a bed porosity of 0.165. The calculated temperature profile that develops with the coalbed after 35 days is shown in figure 9 along with the temperature profile from figure 8. The increased bed compaction results in a smaller temperature rise for the same time period. Associated with the reduction in the bed porosity is a reduction in the bed permeability from 1.69 to 0.14 D. This restricts the flow of oxygen to the zone within the coalbed where heating occurs. The net effect of bed compaction is to moderate the spontaneous heating process.

An increase in particle size has two independent effects upon the heating of a porous coalbed. One effect is to increase the bed permeability, as represented by equation 27. The second effect is to decrease the reaction rate through the inverse dependence of the preexponential factor upon coal particle size. These effects were evaluated through an application of the model equations for particle diameters of 56.25, 112.5, and 225 μm for a fixed bed porosity of 0.33.

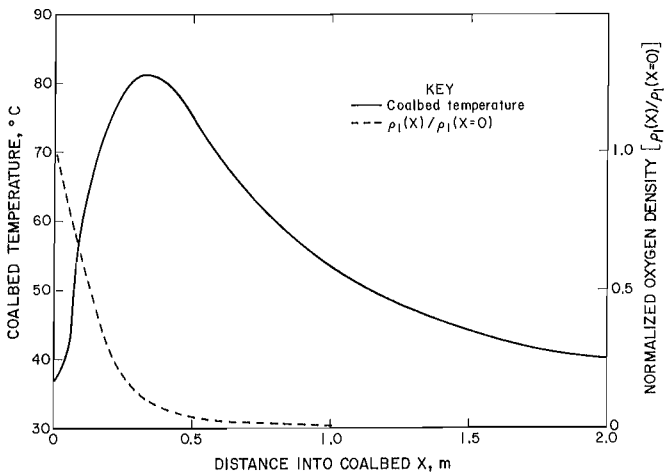

Figure 8.–Calculated coalbed temperature and normalized oxygen density in wind-driven convection model for 10-m-long coalbed, external wind speed of 2.2 m · s^{-1}, coalbed porosity of 0.33, and particle diameter of 56.25 μm after 35 days.

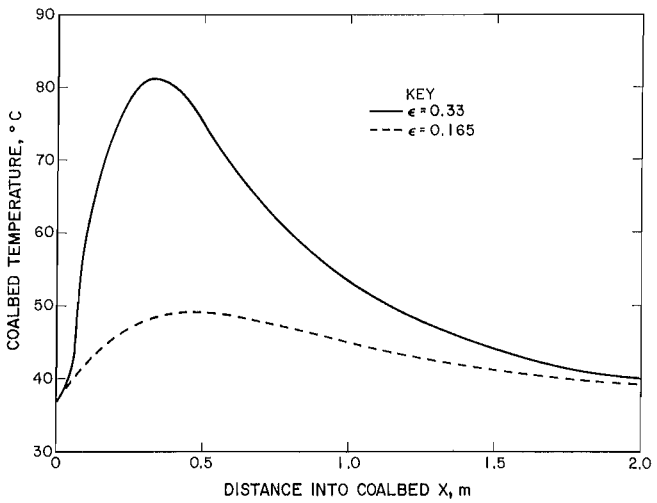

Figure 9.–Calculated coalbed temperature in wind-driven convection model for 10-m-long coalbed, external wind speed of 2.2 m · s^{-1}, particle diameter of 56.25 μm, and coalbed porosities of 0.165 and 0.33 after 35 days.

Table 2 summarizes for these three particle diameters the calculated maximum coalbed temperature and its distance from the wind-driven surface of the coalbed after 27 days. An increase in particle size results, after a fixed elapsed time, in a decrease in the maximum bed temperature and its displacement deeper into the bed. A twofold increase in the particle diameter results in a fourfold increase in the bed permeability, as is shown by equation 27. The increased permeability and the resultant increased interstitial airflow supply oxygen to a greater distance from the surface.

Table 2.–Calculated maximum coalbed temperature and location after 27 days

Coal particle diam (d), μm	Max temp, °C	Location,[1] m
56.25	67	0.35
112.5	48	.5
225	42	.6

[1]Distance from surface of coalbed.

The larger preexponential factor associated with the smaller 56.25-μm-diameter particles resulted in a greater increase in the maximum coalbed temperature over the same period of time, when compared with larger particle diameters of 112.5 and 225 μm, as is evident from table 2. This effect is dominant over any effect imposed by convection for the particle sizes considered.

The effect of particle size upon permeability was decoupled from its effect upon reactivity through a comparison of calculated coalbed temperatures for permeabilities of 1.69 and 6.75 D, while the preexponential factor associated with 56.25-μm-diameter particles was used in each case. The more permeable coalbed yielded a higher calculated temperature for the same elapsed time. If the imposed airflow was sufficiently large, it is expected that convective transport would remove heat.

These calculations demonstrate for the particle sizes and coalbed conditions considered that an increase in particle size has, as a net effect, a decrease in the heat production associated with spontaneous heating and a displacement of the region of maximum heating deeper into the coalbed.

CONCLUSIONS

Three time-dependent mathematical models of spontaneous heating were considered. The first model, with a specified convection of air through a two-dimensional permeable coalbed with an embedded heat source, showed the characteristics expected from spontaneous heating associated with variations in the heat source and the convective velocity. A reasonable match was made of a predicted temperature to the measured temperature profile determined in the experimental program for spontaneous heating at PRC.

The second model, also a time-dependent two-dimensional model, was used to simulate the buoyancy-induced airflow through a partially enclosed porous coalbed with an embedded heat source. The effect of an increase in bed permeability was to enhance the airflow, which, although not preventing the potential for self-heating, did reduce the rate of temperature rise for the reaction kinetics considered.

The third model, a time-dependent one-dimensional model of heat and mass transfer, was of greater utility for a parametric study than the first two models because of the computational efficiency associated with a single space dimension. This model showed that a decrease in coalbed porosity, associated with bed compaction, moderated the self-heating, and that an increase in coal particle size decreased the maximum temperature rise within the coal while moving the zone of maximum heating deeper into the coalbed.

Each of these models should be useful for future analyses of spontaneous heating experiments. These models further provide a framework for the future development of spontaneous heating models that can be adapted for specific spontaneous combustion experiments, as part of the objective for the prediction and control of self-heating in coalbeds.

Future research will include a more precise determination of the reaction rate expression. This requires a detailed analysis of both the oxygen consumption and the temperature rise of a coal sample composed of particles of uniform diameter.

REFERENCES

1. Nordon, P. A Model for the Self-Heating Reaction of Coal and Char. Fuel, v. 58, June 1979, pp. 456-464.

2. Edwards, J. C. Mathematical Modeling of Spontaneous Combustion of Coal. Metall. Soc. AIME, Paper A83-21, 1983, 16 pp.

3. Young, B. D., D. F. Williams, and A. W. Bryson. Two-Dimensional Natural Convection and Conduction in a Packed Bed Containing a Hot Spot and Its Relevance to the Transport of Air in a Coal Dump. Int. J. Heat and Mass Transfer, v. 29, No. 2, 1986, pp. 331-336.

4. Brooks, K., and D. Glasser. A Simplified Model of Spontaneous Combustion in Coal Stockpiles. Fuel, v. 65, Aug. 1986, pp. 1035-1041.

5. Turner, J. S. Buoyancy Effects in Fluids. Cambridge Univ. Press, Cambridge, England, 1973, p. 9.

6. Thorsness, C. B., and S. W. Kang. A General-Purpose, Packed-Bed Model for Analysis of Underground Coal Gasification Processes. Lawrence Livermore Lab., Livermore, CA, 1986, 112 pp.; NTIS: DE86009785/XAB Rep. UCID-20731.

7. Wakao, N., and S. Kaguei. Heat and Mass Transfer in Packed Beds. Gordon and Breach Sci. Publ., New York, 1982, 364 pp.

8. Bischoff, K. B. A Note on Gas Dispersion in Packed Beds. Chem. Eng. Sci., v. 24, 1969, p. 607.

9. Edwards, M. F., and J. F. Richardson. Gas Dispersion in Packed Beds. Chem. Eng. Sci., v. 23, 1968, pp. 109-123.

10. Stott, J. B. The Spontaneous Heating of Coal and the Role of Moisture Transfer (contract JO395146, Univ. Canterbury). BuMines OFR 113-81, 1980, 78 pp.

11. Smith, A. C., and C. P. Lazzara. Spontaneous Combustion Studies of U.S. Coals. BuMines RI 9079, 1987, 28 pp.

12. Streeter, V. L. Handbook of Fluid Dynamics. McGraw-Hill, 1961, p. 168.

13. Bird, R. B., W. E. Stewart, and E. N. Lightfoot. Transport Phenomena. Wiley, 1966, p. 199.

APPENDIX.–NOMENCLATURE

A	preexponential factor, $K \cdot s^{-1}$
C_p	gas specific heat, $cal \cdot g^{-1} \cdot K^{-1}$
C_{ps}	coal specific heat, $cal \cdot g^{-1} \cdot K^{-1}$
d	coal particle diameter, cm
d_1	heating element length, m
d_2	coalbed length, m
D	molecular gas diffusion coefficient, $cm^2 \cdot s^{-1}$
D_k	molecular gas diffusion coefficient in kth direction, $cm^2 \cdot s^{-1}$
$D_k^{(e)}$	effective gas dispersion coefficient in kth direction, $cm^2 \cdot s^{-1}$
E	activation energy, $cal \cdot mol^{-1}$
f	heat flux at solid particle surface, $cal \cdot cm^{-2} \cdot s^{-1}$
g	acceleration due to gravity, 980 $cm \cdot s^{-2}$
h	gas-solid heat transfer coefficient, $cal \cdot cm^{-2} \cdot s^{1} \cdot K^{-1}$
k	gas permeability, cm^2
P	gas pressure, $dyn \cdot cm^{-2}$
P_o	ambient gas pressure, $dyn \cdot cm^{-2}$
Pr	Prandtl number, 1
P_w	heater power, W
Q	heat of reaction of oxygen with coal, $kcal \cdot mol^{-1}$
r	radial coordinate, cm
$\dot{r}$	reaction rate, $g \cdot cm^{-3} \cdot s^{-1}$
R	coal particle average radius, cm
Re	Reynolds number, 1
R_g	gas constant, 8.3143×10^7 $erg \cdot K^{-1} \cdot mol^{-1}$
R_o	heater rod radius, cm
R_1	effective radius of heating element, cm
R_2	coalbed radius, m
S	power source term, $cal \cdot cm^{-3} \cdot s^{-1}$
Sc	Schmidt number, 1
t	time, s
t_r	time for thermal runaway, s
T	gas temperature, K or °C
T_o	ambient temperature, K
T_s	solid temperature, K
u	gas velocity, $cm \cdot s^{-1}$
$\tilde{v}$	interstitial gas velocity, $cm \cdot s^{-1}$
v_k	kth component of superficial gas velocity, $cm \cdot s^{-1}$
$\tilde{v}_k$	kth component of interstitial gas velocity, $cm \cdot s^{-1}$
V	volume of heated region, cm^3
w	wind velocity
W	air molecular weight, $g \cdot mol^{-1}$
x	longitudinal coordinate, cm
y	transverse coordinate, cm
z	axial coordinate, cm

∂ partial derivative, 1

ϵ porosity, 1

λ_g molecular gas thermal conductivity, $cal \cdot cm^{-1} \cdot s^{-1} \cdot K^{-1}$

λ_{go} molecular gas thermal conductivity at ambient temperature, $cal \cdot cm^{-1} \cdot s^{-1} \cdot K^{-1}$

$\lambda_k^{(e)}$ effective thermal conductivity in kth direction, $cal \cdot cm^{-1} \cdot s^{-1} \cdot K^{-1}$

$\lambda_o^{(e)}$ effective thermal conductivity in absence of flow, $cal \cdot cm^{-1} \cdot s^{-1} \cdot K^{-1}$

λ_s particle thermal conductivity, $cal \cdot cm^{-1} \cdot s^{-1} \cdot K^{-1}$

μ gas dynamic viscosity, $g \cdot cm^{-1} \cdot s^{-1}$

π 3.1415927

ρ gas density, $g \cdot cm^{-3}$

ρ_s solid particle density, $g \cdot cm^{-3}$

ρ_1 mass density of oxygen, $g \cdot cm^{-3}$

ρ_{10} mass density of oxygen at ambient condition, $g \cdot cm^{-3}$

Ψ stream function, $g \cdot cm^{-1} \cdot s^{-1}$